Elastic Turbulence in 3D geometries.

Characterising elastic turbulence in viscoelastic fluids at low Reynolds numbers.

R. van Buel, H. Stark, *Institut für Theoretische Physik, Technische Universität Berlin*

In Short

- Elastic turbulence, observed in viscoelastic fluids, enhances heat and mass transport at very low Reynolds numbers.
- The onset of elastic turbulence in a three-dimensional geometry using numerical solutions of the Oldroyd-B model will be investigated.
- Active open-loop control schemes will be applied to the elastic turbulent state in three-dimensional geometries.

Viscoelastic fluids, such as polymeric fluids, have exceptionally useful properties compared to Newtonian fluids. At small scales, viscoelastic fluids exhibit transitions from laminar flows to non-laminar, chaotic and turbulent flows. This is due to *elastic turbulence* [1]. This property is useful for heat and mass transport in flows at the micron scale, where in Newtonian fluids transport is dominated by diffusion. The relevant dimensionless number characterizing viscoelastic fluids is the Weissenberg number Wi, which compares the polymer relaxation time to the characteristic time of the flow dynamics.

Elastic turbulence (see Fig. 1) shows many characteristics similar to inertial turbulence [2]. The fluid flow exhibits a significant increase in flow resistance [3], random fluctuations of fluid velocity that increase with fluid elasticity, intensified mixing of mass, and a broad range of activated temporal or spatial frequencies with power-law scaling [4]. The elastic component of the fluid, quantified by the elastic stress tensor τ, is affected by two processes: stretching of the polymer molecules by velocity gradients and relaxation of elastic stresses. The dominant process depends on the value of the Weissenberg number. At $\mathrm{Wi} \ll 1$ the relaxation of the polymers is much faster than the stretching time due to velocity gradients. The polymer acts like a rigid rod and the fluid flow is Newtonian. For $\mathrm{Wi} > 1$ stretching due to velocity gradients overcomes relaxation. Polymers are considerably elongated [3] and the polymeric stresses grow. This effect is further enhanced by curved streamlines [5,6].

Results of the 3D parallel plate geometry demonstrate impressive qualitative similarities between the numerical solutions of the Oldroyd-B model and experimental results. In Fig. 1 snapshots of the magnitude of the stress tensor and the magnitude of the velocity field are plotted, as well as a snapshot of experimental observations on the same geometry. The order parameter for the three-dimensional parallel plate geometry, defined as the time average of the velocity fluctuations, is shown in fig. 2 as a function of the Weissenberg number. A clear transition from the laminar base flow ($\Phi = 0$) to the occurrence of a secondary flow ($\Phi > 0$) is observed upon increasing the elasticity of the fluid beyond a critical value of $\mathrm{Wi}_c = 1.2$. The transition sets in with a sharp increase in the order parameter which scales as a supercritical pitchfork bifurcation $\Phi \sim (\mathrm{Wi} - \mathrm{Wi}_c)^{1/2}$.

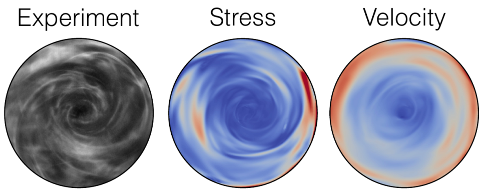

Figure 1: *Snapshots of the turbulent flow (experiment [1]) as well as stress and velocity fields from numerical solutions of the Oldroyd-B model.*

Recently, we investigated applying an active open-loop control scheme to the elastic turbulent state of a viscoelastic fluid in a two-dimensional Taylor-Couette geometry [7]. We have shown a transition to elastic turbulence at $\mathrm{Wi} = 10$ in earlier work, where we applied a shear rate constant in time in the same geometry [8]. By applying time-modulated shear rates, a form of active open-loop control, elastic turbulence is reduced. The Deborah number is determined by the rate of change in the shear flow and thus is given by the ratio of the relaxation rate of the fluid over the modulation frequency. We obtain numerical solutions of the Oldroyd-B model and use two kinds of time-modulated shear rates in the form of a square or sine wave, which display similar results. Elastic turbulence decreases upon increasing the modula-

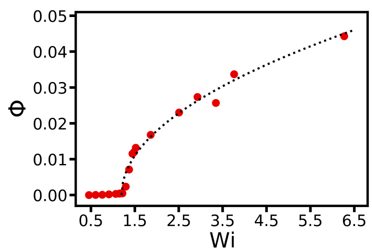

Figure 2: *Order parameter Φ, defined as the time average of the velocity fluctuations, as a function of the Weissenberg number Wi. The dotted line shows the scaling law $(\mathrm{Wi} - \mathrm{Wi}_c)^{1/2}$ with $\mathrm{Wi}_c = 1.2$.*

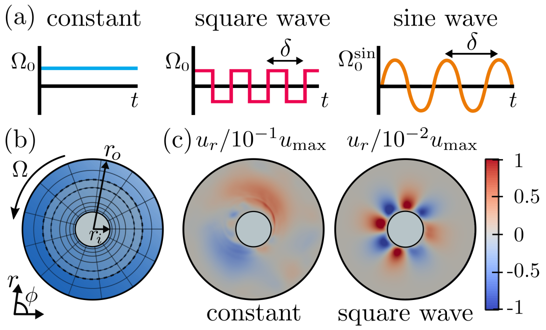

Figure 3: *(a) Angular velocity Ω versus time of the outer cylinder for different driving protocols. (b) Schematic of the 2D Taylor-Couette geometry. The outer cylinder rotates with the angular velocity Ω. (c) Color-coded radial velocity field component u_r normalized by the maximum velocity u_{max} for $\mathrm{Wi} = 21.4$. Left: at time $t = 225$ s, where Ω is constant. Right: at $t = 375$ s after the square-wave modulated driving with $\mathrm{De} = 0.28$ has been switched on.*

tion frequency and ultimately vanishes at a critical Deborah number De_c. Here, the flow field assumes the radially symmetric base flow of the non-turbulent case.

The order parameter Φ sharply increases above a critical (inverse) Deborah number De_c^{-1}, which depends on the Weissenberg number Wi, see Fig. 4. The transition displays a square-root scaling, $(\mathrm{De}^{-1} - \mathrm{De}_c^{-1})^{1/2}$, implying that the transition is supercritical. This result is further tested by applying the modulated driving directly to the rest state (open square symbols for $\mathrm{Wi} = 21.4$ in Fig. 4). The different initial conditions do not lead to different values of Φ, corresponding to a supercritical transition. Another striking feature is that the order parameter displays universal behavior around the transition. Indeed, as the inset of Fig. 4 demonstrates, all curves for different Wi fall on a single master curve when we normalize Φ by $\mathrm{Wi}^{3/2}$ and plot them versus

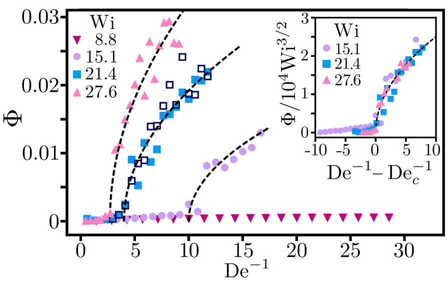

Figure 4: *Order parameter Φ as a function of the inverse Deborah number $\mathrm{De}^{-1} = \delta/\lambda$ in the case of square wave modulations for four Weisenberg numbers. The time average of the secondary-flow strength is taken over at least 500 rotations in the turbulent regime; after the flow has been driven for 250 rotations with a constant velocity. Open blue squares: the modulated driving starts from the beginning. The dashed lines are square root fits to $\Phi \sim \sqrt{\mathrm{De}^{-1} - \mathrm{De}_c^{-1}}$. Inset: the rescaled data collapse onto a single master curve.*

$\mathrm{De}^{-1} - \mathrm{De}_c^{-1}$.

In this project we plan to expand active open-loop control schemes applied to elastic turbulence in viscoelastic fluids to 3D geometries using the same approach as for the 2D case described above. Thereby we provide an important step towards applying further active control strategies to viscoelastic fluids. By modulating the shear rate of a two-dimensional Taylor-Couette flow, we have been able to control the onset of elastic turbulence. Our earlier work demonstrates how sensitive elastic turbulence is to oscillating shear. Based on the strong similarities observed in the order parameter of the two and three-dimensional flows, we would like to expand our analysis of active open-loop control to fully three-dimensional simulations. We will concentrate on two exemplary 3D geometries: the van Karman swirling flow in a parallel-plate geometry and the Taylor-Couette geometry. Through this work, we hope to inspire further experimental and theoretical investigations on active open-loop or feedback control of viscoelastic fluid flow, for example, in microfluidic systems.

WWW

http://www.itp.tu-berlin.de/stark/

More Information

[1] A. Groisman and V. Steinberg, *Nature* **405**, 53 (2000). doi:10.1038/35011019

[2] A. Groisman and V. Steinberg, *New J. Phys.* **6**, 29 (2004). doi:10.1088/1367-2630/6/1/029

[3] J. L. Lumley, *Journal of Polymer Science: Macromolecular Reviews*, **7** 263 (1973). doi:10.1002/pol.1973.230070104

[4] M. Grilli, A. Vázquez-Quesada, and M. Ellero, *Phys. Rev. Lett.* **110**, 174501 (2013). doi:10.1103/PhysRevLett.110.174501

[5] P. Pakdel and G. H. McKinley, *Phys. Rev. Lett.* **77**, 2459 (1996). doi:10.1103/PhysRevLett.77.2459

[6] A. Fouxon and V. Lebedev, *Phys. Fluids.* **15**, 2060 (2003). doi:10.1063/1.1577563

[7] R. van Buel, and H. Stark, *arXiv preprint arXiv:1912.06950* (2019).

[8] R. van Buel, C. Schaaf, H. Stark, *Europhys. Lett.* **124**, 14001 (2018). doi:10.1209/0295-5075/124/14001

Funding

Sonderforschungsbereich (SFB) 910